Exploiting nonlinear propagation in echo sounders and sonar

Fabrice Prieur[1], Sven Peter Näsholm[1], Andreas Austeng[1], Sverre Holm[1]

[1]Department of Informatics, University of Oslo, P.O. Box 1080, NO-0316 Oslo, Norway, {**fabrice,svenpn,andrea,sverre**}**@ifi.uio.no**

Mainstream sonars transmit and receive signals at the same frequency. As water is a nonlinear medium, a propagating signal generates harmonics at multiples of the transmitted frequency. For sonar applications, energy transferred to higher harmonics is seen as a disturbance. To satisfy requirements for calibration of echo sounders in fishery research, input power has to be limited to avoid energy loss to harmonics generation. Can these harmonics be used in sonar imaging? The frequency dependency of target echos, and the different spatial distribution of higher harmonics can contribute to additional information on detected targets in fish classification, ocean bathymetry, or bottom classification. Our starting point was the sonar equation adapted for the second harmonic. We have simulated nonlinear propagation of sound in water, and obtained estimates of received pressure levels of harmonics for a calibration sphere, or a fish as reflector. These pressure profiles were used in the sonar equation to compare harmonics to fundamental signal budget. Our results show that a 200 kHz thermal noise limited echo sounder, with a range of 800 m will reach around 300 m for the second harmonic. This means the second harmonic is useful in many applications.

1 Introduction

Non-linear propagation of ultrasound was identified many years ago as a phenomenon that potentially may be utilized for acoustic imaging improvement. Already in 1965, Berktay [1] mentioned several possible uses of non-linearity in underwater imaging applications. When transmitting two simultaneous waves with slightly different frequencies, theory [2] predicts that due to non-linearity, secondary waves are generated at frequencies around the sum as well as the difference of the two transmitted frequencies. This property is used by parametric sonars.

In acoustic medical imaging, non-linear scattering from contrast agents was first used to enhance some imaging features. Then second harmonics generated by non-linear propagation in tissue without contrast agent were found to increase image quality, giving birth to the tissue harmonic imaging mode (THI) [3]. Duck [4] gave a good review explaining why the second harmonic used in THI has properties beneficial for image quality.

Non-linear propagation as it naturally occurs when sound propagates in water, is in sonar applications mainly considered as a disturbance that perturbs target strength evaluation [5]. However, a question that naturally occurs is: *"Can non-linear propagation be made use of in sonar application in a similar manner as in tissue harmonic medical imaging?"*. Experimental proofs were presented already in 1980 [6] but since then, little has been published on second harmonic imaging in underwater acoustic imaging.

We have applied the widely accepted definition of the sonar budget equation [7] to the simulated second harmonic generated during non-linear propagation in water. The resulting sonar budget equation predicts that this second harmonic may be used in sonar imaging, just like the fundamental waves at the transmit frequencies. Given that benefits of THI in medical imaging are valid also in underwater imaging, it is expected that second harmonic imaging would give rise to enhanced directivity, and reduced sidelobes compared to fundamental imaging.

In this paper, each term of the sonar equation have been adapted to the second harmonic to generate a sonar equation for propagation in the non-linear regime. We have run numerical simulations in order to compare the range limits for the second harmonic and for the fundamental.

2 Sonar equation overview

2.1 Equation for target detection

The derivation of the sonar budget equations follows the presentation in [7]. When assuming isotropic noise as perturbation source for target detection, the model equation is:

$$SL - 2TL + TS = NL - DI + DT. \tag{1}$$

It characterizes the case of the monostatic sonar. The meaning and definitions of the terms in Eq. (1) are summarized in Table 1 which is reproduced from [7].

2.2 Directivity index – DI

In the case of a signal as a perfectly coherent unidirectional plane wave, and an isotropic noise, the array gain of the transducer (AG) is the directivity index. This assumption will be valid in our case since at reception, the signal received is in its far field, and can be considered as a plane wave; and at transmission after 1 m, the wave generated by the piston can be considered plane.

Parameter		Reference	Definition
Source level	SL	1m from source on its acoustic axis	$10\log\frac{\text{intensity of source}}{\text{reference intensity}^*}$
Transmission loss	TL	1m from source and at target or receiver	$10\log\frac{\text{signal intensity at 1 m}}{\text{signal intensity at target or receiver}}$
Target strength	TS	1m from acoustic center of target	$10\log\frac{\text{echo intensity at 1 m from target}}{\text{incident intensity}}$
Noise level	NL	at hydrophone location	$10\log\frac{\text{noise intensity}}{\text{reference intensity}^*}$
Receiving directivity index	DI	at hydrophone terminals	$10\log\frac{\text{noise power generated by an equivalent nondirectional hydrophone}}{\text{noise power generated by actual hydrophone}}$
Detection threshold	DT	at hydrophone terminals	$10\log\frac{\text{signal power to just perform a certain function}}{\text{noise power at hydrophone terminals}}$

*The reference intensity is that of a plane wave of rms pressure 1 μPa.

Table 1: Definitions of terms used in the sonar equation (reproduced from [7]).

In our case, the receiver is the same as the transmitter; a circular piston. Therefore, it has axial symmetry. For an array/aperture steered in the direction of the signal we have:

$$AG = DI = 10\log\frac{4\pi}{2\pi\int_{-\pi/2}^{\pi/2} b(\theta)\cos(\theta)\mathrm{d}\theta}, \qquad (2)$$

where $b(\theta)$ is the beam pattern of the aperture.
For a circular piston of radius R, the beam pattern is:

$$b(\theta) = \left(\frac{2J_1[(2R\pi/\lambda)\sin(\theta)]}{(2R\pi/\lambda)\sin(\theta)}\right)^2, \qquad (3)$$

where J_1 is the Bessel function of order one, and λ is the wavelength of the signal. Eq. (3) combined with Eq. (2) give the directivity index

$$DI = 10\log\left(\left(\frac{2R\pi}{\lambda}\right)^2\right). \qquad (4)$$

2.3 Source Level – SL

The source level is simply found by calculating the ratio between the intensity at 1 m, and the reference intensity (1μPa rms). The equations become:

$$I_{1\mathrm{m}} = \frac{\overline{p}_{1\mathrm{m}}^2}{\rho c} = \frac{p_{1\mathrm{m}}^2}{2\rho c}, \quad \text{and} \quad I_{\text{ref}} = \frac{\overline{p}_{\text{ref}}^2}{\rho c} = \frac{1\mu\text{Pa}^2}{\rho c}, \qquad (5)$$

giving

$$SL = 10\log\left(\frac{I_{1\mathrm{m}}}{I_{\text{ref}}}\right) = 10\log\left(\frac{\overline{p}_{1\mathrm{m}}^2}{1\mu\text{Pa}^2}\right). \qquad (6)$$

This method is valid for the second harmonic if the bulk of the energy transferred from the fundamental to the second harmonic happens over a short propagation distance (much less than one meter). This is the case in our simulations. If, after one meter, the second harmonic is still building up, $\overline{p}_{1m}$ should not be used to calculate the SL. Instead, an equivalent level should be calculated.

2.4 Transmission Loss – TL

In order to compute transmission losses, non linear propagation is simulated taking in account diffraction, and damping in water. For each harmonic, transmission losses are computed as follows:

$$TL = 10\log(p_{1\mathrm{m}}^2/p_r^2), \qquad (7)$$
p_r: reflected pressure at target,
$p_{1\mathrm{m}}$: pressure at 1 m.

2.5 Target Strength – TS

In our simulations, two types of reflector have been used. The first type is a perfect sphere, and the second is a fish. In the first case, a sphere of radius a that reflects all the incident energy that reaches it, is considered. This is a typical calibration sphere. For such a reflector, incident plane wave energy is the product of the incident intensity by the area built by the projection of the sphere onto the wave plane. The reflected wave is spherical and its energy spreads over 4π steradians. The formula for the reflected intensity without attenuation at a distance r from the sphere center (acoustic center) is:

$$I_r = \frac{\pi a^2 I_i}{4\pi r^2}, \quad I_i\text{: incident intensity.} \qquad (8)$$

Hence the formula for the TS:

$$TS = 10\log\frac{I_r}{I_i}\Big|_{r=1\text{ m}} = 10\log\frac{a^2}{4(1\text{ m})^2}. \qquad (9)$$

In the second case, the target strength formula is based on empirical measurements [7] exhibiting a large dependence on the size of the fish:

$$TS = 19.1\log L - 0.9\log F - 62, \qquad (10)$$
L: size of fish in cm, $\quad F$: frequency.

Eqs. (9), and (10) are the expressions for the TS that will be used in the simulations. These expressions are valid when sound diffraction by target is negligible compared to reflection. This can be translated for the sphere into inequality $ka > 10$, where $k = 2\pi/\lambda$ is the received pulse wavenumber, and λ its wavelength, and by $L >> \lambda$ for the fish.

2.6 Detection threshold – DT

For the case of an active sonar where the target processor is a cross-correlator, the detection threshold is defined as [7]:

$$DT = 10 \log \frac{d}{2\tau}, \quad (11)$$

d: detection index, τ: pulse duration.

In the simulation, the detection index d will characterize a detection probability of 50% and a false alarm probability of 0.01%. Fig. 12.7 in [7] was used to determine d.

2.7 Noise Level – NL

Ambient noise level seems to be very variable. It depends on the depth at which the receiver is placed, on the state of the sea, on the wind speed, on the shipping traffic, and if the sea is deep or shallow. In our case, the noise generated for the frequency range of interest is mainly due to thermal noise originating in the molecular motion of the sea. The chosen model valid for frequencies above 100 kHz is:

$$NL = -15 + 20 \log(F/1 \text{ kHz}), \quad (12)$$

F: frequency of considered wave.

Note that $NL - DI$ is constant with frequency (see Eq. (4)). DT being independent of frequency, the quantity $NL - DI + DT$ will be equal for fundamental and second harmonic.

3 Nonlinear propagation simulations to estimate the sonar equation parameters

3.1 Method and parameters

Simulations were carried out using our implementation of an angular spectrum method to solve Burgers' equation [8]. The angular spectrum method operates in the frequency domain and consists of two substeps. The first is a nonlinear step which involves Burgers' equation and takes care of coupling between the harmonics. In the second step, diffraction and absorption in the linear domain are taken care of for all harmonics. In this way a number of harmonics are propagated in the direction of propagation.

In order to obtain the pressure field at a depth r, following Christopher and Parker [9], the radial extent of the simulation was set to $T = 4.5 \tan\theta \cdot r$, where $\theta = 9^\circ$ represents the opening angle of the calculated field at depth r. Such a value of T ensures no perturbation from source replica. The number of radial samples was set to $N = 2T/\lambda$ where λ is the wavelength. The propagation step size in depth dr was set to 5 mm. The diffraction step was computed in the frequency domain using the ray theory-updated frequency sampled convolution (RFSC) [9]. Attenuation is applied at each step for all harmonics using the formula:

$$p_n(m+1) = p_n(m) \cdot \exp[-\alpha \cdot (n \cdot F_0/10^6)^2 \cdot dr], \quad (13)$$

where $p_n(m)$ is the pressure of the nth harmonic at depth $m \cdot dr$, α is the attenuation coefficient in Np/MHz^2/m, and F_0 is the fundamental frequency of the wave. The nonlinear substep is given by Christopher and Parker [10], but since we work with the real amplitude or one-sided spectrum [11], we have used twice the constant in the nonlinear substep (Eq. (3) in [10]). In all simulations using the angular spectrum method, 50 harmonics were used.

The simulations are done when a circular piston is used as source and receiver, and the reflector is a calibration sphere or a fish. The water density and sound speed are assumed to be constant. The parameters of the simulation are summed up in Table 2. Simulations are based on a Simrad ES200-7C transducer, and a EK60 echo sounder. Non-linear propagation is simulated to a depth of $r_0 = 10$ m. At deeper depths than this, the amplitude is low enough to allow linear propagation of the remaining fundamental and the accumulated second harmonic. The formula used to simulate linear propagation at range r is shown in Eq. (14)

$$p_n(r) = p_n(r_0)\frac{r_0}{r} \exp[-\alpha \cdot (n \cdot F_0/10^6)^2 \cdot (r - r_0)]. \quad (14)$$

Parameter	Value
Source radius, R	31.5 mm
Target radius, a	38.1 mm
Frequency, F_0	200 kHz
Pulse duration, τ	0.1 ms
Input RMS pressure, $\overline{p}_0$	580 kPa
Water density, ρ	998 kg/m^3
Sound speed, c	1479 m/s
Nonlinearity coefficient, β	3.49
Fish size, L	25 cm
Attenuation, α	0.025 Np/MHz^2/m
Detection index, d	15

Table 2: Parameters used in simulation.

3.2 Results

Sphere as a reflector

In the first case of the spherical reflector, the simulations are run using the ASA [9, 10] (Angular Spectrum Approach) assuming axial symmetry (Hankel transform was used).

Figs. 1 and 2 show the axial pressure profiles, and the transmission budget for the the fundamental and the second harmonic to a depth of 3 km. The round and square markers at the top are the source levels (SL) for fundamental and second harmonic, the horizontal line at the bottom corresponds to $NL - DI + DT$, and the decreasing curves correspond to $SL - 2TL + TS$. Table 3 sums up the computed values in dB.

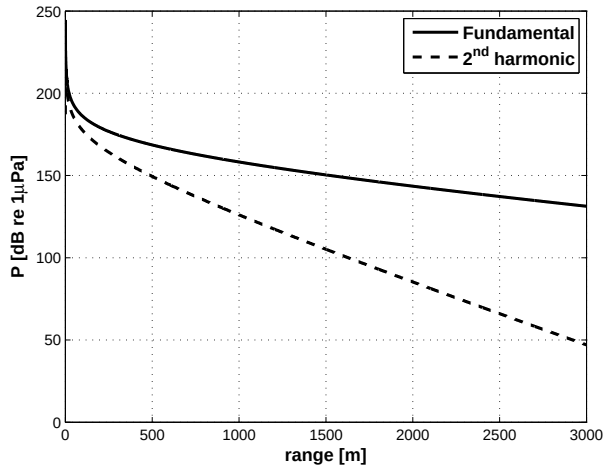

Figure 1: Axial profiles for first and second harmonics.

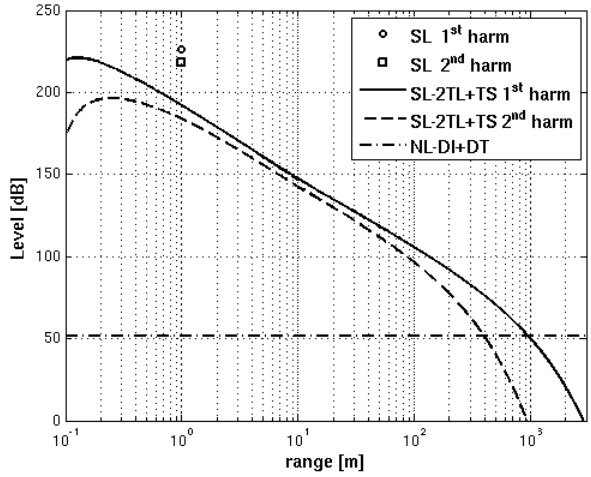

Figure 2: Sonar equation transmission budget plots in the case of a spherical reflector.

	SL	TS	DI	DT	NL	TL
1^{st} harm.	226.3	-34.4	28.6	48.8	31.0	98.0
2^{nd} harm.	218.1	-34.4	34.6	48.8	37.0	174.1

Table 3: Computed values using the ASA.

The noise level (NL) and the directivity index (DI) both increase by the same amount (6 dB) between the fundamental and the second harmonic. This explains why $NL-DI+DT$ is constant for fundamental and second harmonic.

Fish as reflector

In the case where the target is a fish, the same simulations are run. The axial pressure profile is the same as shown in Fig. 1. Fig. 3 shows the sonar equation transmission budget in this case. The round and square markers at the top are the source levels (SL) for fundamental and second harmonic, the horizontal line at the bottom corresponds to $NL - DI + DT$, and the decreasing curves correspond to $SL - 2TL + TS$.

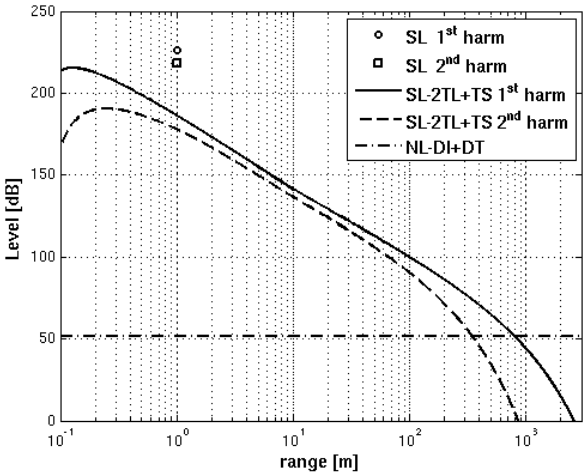

Figure 3: Sonar equation transmission budget plots in the case of a fish as a reflector

The only difference in the computed values from Table 3, is the target strength that dropped from -34.4 dB to -40.1 dB for the fundamental frequency and -40.3 dB for the second harmonic.

4 Summary

With the given simulation parameters, if the fundamental frequencies are used, they can detect a spherical reflector and a fish down to approximately 960 m and 800 m respectively. If instead the second harmonic that is accumulated during propagation in the non-linear regime is utilized for detection, the simulations predict a spherical reflector and a fish to be detectable at 400 m and 340 m respectively. These estimates indicate that second harmonic can be used for target detection providing the range is down-graded accordingly when compared to fundamental imaging. Imaging using second harmonic, in turn, offers better resolution and lower sidelobe levels.

Combination of fundamental and second harmonic imaging seems also possible in ranges below 340 m, giving target echos at two widely separated frequencies. This should help in target recognition as discussed by Korneliussen and Ona [12].

References

[1] H. O. Berktay. Possible exploitation of non-linear acoustics in underwater transmitting applications. *Journal of Sound Vibration*, 2(4):435–461, 1965.

[2] Peter J. Westervelt. Scattering of sound by sound. *J. Acoust. Soc. Amer*, 29(2):199–203, February 1957.

[3] James. D. Thomas and David. N. Rubin. Tissue harmonic imaging: Why does it work? *Journal of the American Society of Echocardiography*, 11(8):803–808, 1998.

[4] Francis. A. Duck. Nonlinear acoustics in diagnostic ultrasound. *Ultrasound in Med. & Biol.*, 28(1):1–18, 2002.

[5] F. E. Tichy, H. Solli, and H. Klaveness. Non-linear effects in a 200-kHz sound beam and the consequences for target-strength measurement. *ICES Journal of Marine Science*, 60:571–574, 2003.

[6] T.G. Muir. Nonlinear effects in acoustic imaging. *Acoustical imaging*, 9:93–109, 1980.

[7] Robert. J. Urick. *Principles of underwater sound*. McGraw-Hill Book Company, third edition, 1983.

[8] J.-F. Synnevåg and S. Holm. Non-linear propagation of limited diffraction beams. pages 1885–1888, Sendai, Japan, October 1998.

[9] P. T. Christopher and K. J. Parker. New approaches to the linear propagation of acoustic fields. *J. Acoust. Soc. Amer*, 90(1):507–521, July 1991.

[10] P. T. Christopher and K. J. Parker. New approaches to nonlinear diffractive field propagation. *J. Acoust. Soc. Amer*, 90(1):488–499, July 1991.

[11] D. H. Trivett and A. L. Van Buren. Comments on "Distortion of finite amplitude ultrasound in lossy media,"by M. E. Haran and B. D. Cook [J. Acoust. Soc. Am. 73, 774-779 (1983)]. *J. Acoust. Soc. Amer*, 76(4):1257–1258, October 1984.

[12] R.J. Korneliussen and E. Ona. Synthetic echograms generated from the relative frequency response. *ICES Journal of Marine Science*, 60(3):636–640, 2003.